

General Relativistic Augmentation of Neutrino Pair Annihilation Energy Deposition Near Neutron Stars

Jay D. Salmonson^{1,2} and James R. Wilson

Lawrence Livermore National Laboratory, Livermore, CA 94550

ABSTRACT

General relativistic calculations are made of neutrino-antineutrino annihilation into electron-positron pairs near the surface of a neutron star. It is found that the efficiency of this process is enhanced over the Newtonian values up to a factor of more than 4 in the regime applicable to Type II supernovae and by up to a factor of 30 for collapsing neutron stars.

Subject headings: neutrinos—radiative transfer—stars:supernovae

1. Introduction

It has long been realized that the reaction $\nu + \bar{\nu} \rightarrow e^+ + e^-$, near the surface of a hot neutron star, is of considerable importance to type II supernova dynamics. At late times, in particular, several percent of the neutrino luminosity ($L_\nu \sim 10^{52}$ ergs/sec) from the hot protoneutron star is deposited into the stellar envelope via $\nu\bar{\nu} \rightarrow e^+e^-$ and neutrino-lepton scattering. This energy deposition, together with neutrino-baryon capture, significantly augments the neutrino heating of the envelope in a successful supernova via the so-called “delayed shock mechanism” (Bethe & Wilson 1985, Bethe 1990). The late time heating of the envelope is most important for the r-process nucleosynthesis.

Another case of interest stems from neutron star collapse. This could occur either from accretion (Bhattacharya & van den Heuvel 1991) directly from a companion or from plunging into the interior of a companion (Fryer, Benz & Herant 1996). A third possibility is suggested in recent studies of close neutron star binaries near their last stable orbit (Wilson et al. 1996, Mathews & Wilson 1997). This work indicates that neutron stars in such

¹Department of Applied Science, University of California, Davis, CA 95616

²e-mail: salmonson@llnl.gov

systems can compress, heat and emit a neutrino luminosity as high as 10^{53} ergs/second. A fraction of these neutrinos should be converted to e^+e^- pairs via $\nu\bar{\nu} \rightarrow e^+e^-$. In all of these scenarios, understanding the efficiency of this reaction is crucial to modeling the energy dynamics and observable emission, such as the formation of gamma-ray bursts.

Previous calculations of reaction efficiencies near neutron stars have been based upon Newtonian gravity (Goodman, Dar & Nussinov 1987, Cooperstein, van den Horn & Baron 1986); i.e. they assume $\frac{2GM}{c^2 R} \ll 1$ where M is the gravitational mass of the neutron star and R is the distance scale. In fact $\frac{2GM}{c^2 R}$ can be ~ 0.4 for supernova calculations and ~ 0.7 for collapsing neutron stars (Mathews & Wilson 1997) and the effects of gravity cannot be ignored.

In this paper we develop a relativistic analytical model to compute the efficiency of $\nu\bar{\nu} \rightarrow e^+e^-$ in a high-gravity environment such as near a neutron star. We find that relativistic enhancements to the Newtonian reaction rate can be large; up to factors of 10.

2. Neutrino Annihilation

Newtonian calculations of the $\nu\bar{\nu} \rightarrow e^+e^-$ energy deposition rate near a hot neutron star were done by Cooperstein, van den Horn & Baron (1986) and Goodman, Dar & Nussinov (1987). The energy deposition per unit time, per volume (Goodman *et al.* 1987) is

$$\dot{q}(r) = \iint f_\nu(\mathbf{p}_\nu, r) f_{\bar{\nu}}(\mathbf{p}_{\bar{\nu}}, r) \{ \sigma |\mathbf{v}_\nu - \mathbf{v}_{\bar{\nu}}| \varepsilon_\nu \varepsilon_{\bar{\nu}} \} \varepsilon_\nu + \varepsilon_{\bar{\nu}} \varepsilon_\nu \varepsilon_{\bar{\nu}} d^3\mathbf{p}_\nu d^3\mathbf{p}_{\bar{\nu}} \quad (1)$$

where f_ν and $f_{\bar{\nu}}$ are number densities in phase space, \mathbf{v}_ν is the neutrino velocity, and σ is the rest frame cross section. The term in curly brackets in equation (1) is Lorentz invariant. Thus it can be calculated in the center-of-mass frame to be

$$\{ \sigma |\mathbf{v}_\nu - \mathbf{v}_{\bar{\nu}}| \varepsilon_\nu \varepsilon_{\bar{\nu}} \} = DG_F^2 c 3\pi (\varepsilon_\nu \varepsilon_{\bar{\nu}} - \mathbf{p}_\nu \cdot \mathbf{p}_{\bar{\nu}} c^2)^2, \quad (2)$$

with $G_F^2 = 5.29 \times 10^{-44} \text{ cm}^2 \text{ MeV}^{-2}$ and

$$D = 1 \pm 4 \sin^2 \theta_W + 8 \sin^4 \theta_W. \quad (3)$$

Here $\sin^2 \theta_W = 0.23$ and the $+$ sign is for $\nu_e \bar{\nu}_e$ pairs, while $-$ is for $\nu_\mu \bar{\nu}_\mu$ and $\nu_\tau \bar{\nu}_\tau$ pairs. Note that we have assumed that the mass of the electrons is negligible since, for the applications of interest, the energy of the neutrinos is greater than 10 MeV. Now we replace $\mathbf{p}_\nu c = \varepsilon_\nu \boldsymbol{\Omega}_\nu$

and $d^3\mathbf{p}_\nu = \frac{\varepsilon_\nu^2}{c^3} d\varepsilon_\nu d\Omega_\nu$ where Ω_ν is the unit direction vector and $d\Omega_\nu$ is a solid angle

$$\dot{q} = DG_F^2 3\pi c^5 \Theta(r) \iint f_\nu f_{\bar{\nu}} (\varepsilon_\nu + \varepsilon_{\bar{\nu}}) \varepsilon_\nu^3 d\varepsilon_\nu \varepsilon_{\bar{\nu}}^3 d\varepsilon_{\bar{\nu}} , \quad (4)$$

where the angular integrations are represented by

$$\Theta(r) \equiv \iint (1 - \Omega_\nu \cdot \Omega_{\bar{\nu}})^2 d\Omega_\nu d\Omega_{\bar{\nu}} . \quad (5)$$

Thus the energy and angular dependencies have been separated. The energy integrals can then be performed in their local frame. Taking $f_\nu = 2h^3(e^{\varepsilon_\nu/kT} + 1)^{-1}$ for fermions

$$\int_0^\infty f_\nu \varepsilon_\nu^3 d\varepsilon_\nu = 2(kT)^4 h^3 7\pi^4 120 \quad (6)$$

$$\int_0^\infty f_\nu \varepsilon_\nu^4 d\varepsilon_\nu = 2(kT)^5 h^3 45\zeta(5)2 \quad (7)$$

we finally get

$$\dot{q} = 7DG_F^2 \pi^3 \zeta(5) 2c^5 h^6 (kT)^9 \Theta(r) \propto T(r)^9 \Theta(r) \quad (8)$$

where $T(r)$ is the temperature measured by a local observer. All calculations carried out thus far are in the local frame. In order to complete the evaluation of $T(r)$ and $\Theta(r)$, gravitational redshift and path bending must be included.

It is also of interest to calculate the radial momentum density \dot{p} imparted to the e^+e^- plasma from the $\nu\bar{\nu}$ luminosity. This is related to the energy deposition of Equation (8) by

$$\dot{p} = \dot{q} c \Phi_p(r) \Theta(r) \quad (9)$$

where

$$\Phi_p(r) \equiv 12 \iint (1 - \Omega_\nu \cdot \Omega_{\bar{\nu}})^2 (\hat{\mathbf{r}} \cdot (\Omega_\nu + \Omega_{\bar{\nu}})) d\Omega_\nu d\Omega_{\bar{\nu}} \quad (10)$$

and $\hat{\mathbf{r}}$ is the unit vector normal to the stellar surface.

3. Bending of Null Geodesics

From Misner, Thorne & Wheeler, the path of a zero mass particle, a null geodesic, in Schwarzschild coordinates is given by

$$\left(1r^2drd\phi\right)^2 + 1 - 2M/r = b^2, \quad (11)$$

where r is the distance from the origin, ϕ is the longitude, and b is the impact parameter. Here the neutron star mass M is expressed in units of distance; i.e. $Gc^2 = 1$. All other units are in cgs. We wish to express Equation (11) in terms of the angle θ between the particle trajectory and the tangent vector to a circular orbit. In terms of local radial and longitudinal velocities $v_{\hat{r}}$ and $v_{\hat{\phi}}$ this becomes

$$\tan \theta = v_{\hat{r}}/v_{\hat{\phi}} = \sqrt{|g_{rr}|}drd\lambda/\sqrt{|g_{\phi\phi}|}d\phi d\lambda = r\sqrt{1-2M/r}drd\phi. \quad (12)$$

This expression can be substituted into Equation (11) and simplified to give

$$b = r \cos \theta_r \sqrt{1 - 2M/r}. \quad (13)$$

All points along a single orbit will share the same impact parameter. Thus a particle emanating from the photosphere at R with a trajectory denoted by θ_R will have a trajectory θ_r at radius r given by

$$\cos \theta_r = Rr\sqrt{1 - 2M/r} \cos \theta_R. \quad (14)$$

It is interesting to note that this equation implies a minimum photosphere radius, i.e. $R_{min} = 3M$, below which a massless particle (neutrino) emitted tangent to the stellar surface ($\theta_R = 0$) is gravitationally bound. The present discussion is restricted to the domain $R > 3M$.

We may now evaluate Equation (5). Defining $\mu = \sin \theta$, then $\Omega = (\mu, \sqrt{1 - \mu^2} \cos \phi, \sqrt{1 - \mu^2} \sin \phi)$ and $d\Omega = \cos \theta d\theta d\phi$ we get

$$\Theta(r) = 4\pi^2 \int_x^1 \int_x^1 [1 - 2\mu_\nu \mu_{\bar{\nu}} + \mu_\nu^2 \mu_{\bar{\nu}}^2 + 12(1 - \mu_\nu^2)(1 - \mu_{\bar{\nu}}^2)] d\mu_\nu d\mu_{\bar{\nu}}, \quad (15)$$

where we define

$$x \equiv \sqrt{1 - \left(\frac{R}{r}\right)^2 1 - 2Mr 1 - 2MR} . \quad (16)$$

The result is

$$\Theta(r) = 2\pi^2 3(1-x)^4(x^2 + 4x + 5) . \quad (17)$$

In the Newtonian limit ($M \rightarrow 0$) this function has the same form as that in Goodman, Dar & Nussinov (1987) and Cooperstein, van den Horn & Baron (1987). In the limit $r \gg R$ this becomes $\Theta(r) \approx \pi^2 2(Rr)^8$, so the efficiency of this process falls off strongly with radius as the streaming particle trajectories become more parallel.

For the momentum density deposition, the integration of Equation (10) is similarly performed and the result is

$$\Phi_p(r) = \pi^2 6(1-x)^4(8 + 17x + 12x^2 + 3x^3) . \quad (18)$$

Thus at the surface of the star ($r = R$) we have $\Phi_p(r)\Theta(r) = 25$ and the deposited e^+e^- plasma moves with a high momentum. At large distances, as $r \rightarrow \infty$, then $\Phi_p(r)\Theta(r) \rightarrow 1$, as expected.

3.1. Gravitational Redshift

The temperature $T(r)$ in Equation (8) is the neutrino temperature at radius r . This must be put in terms of an observable quantity such as the observed luminosity L_∞ . To do this we start by expressing the temperature of the free streaming neutrinos at radius r in terms of their temperature at the neutrinosphere radius R using the appropriate gravitational redshift. Temperature, like energy, varies linearly with redshift

$$T(r) = \sqrt{1 - 2MR 1 - 2Mr} T(R) . \quad (19)$$

The luminosity varies quadratically with redshift

$$L_\infty = (1 - 2MR)L(R) , \quad (20)$$

and at the neutrinosphere, the local neutrino luminosity for a single neutrino species is

$$L(R) = L_\nu + L_{\bar{\nu}} = 4\pi R^2 \cdot 74ac4T(R)^4 . \quad (21)$$

Combining these, Equation (8) becomes

$$\begin{aligned} \dot{q} &= 7DG_F^2\pi^3\zeta(5)2c^5h^6k^9\left(\frac{7}{8}\pi ac\right)^{-9/4} L_\infty^{9/4} \\ &\times \Theta(r) \left(\sqrt{1-2Mr} - 2Mr \right)^{9/2} R^{-9/4} . \end{aligned} \quad (22)$$

Equation (22) describes the idealized energy deposition in e^+e^- pairs from the reaction $\nu + \bar{\nu} \rightarrow e^+ + e^-$ at radius r above a neutron star of radius R and with a neutrino luminosity L_∞ . The momentum density deposition is still described by Equation (9).

4. Results

In order to quantify the total e^+e^- pair energy deposition, we define \dot{Q} as the integral of \dot{q} , given by Equation (22), over proper volume. \dot{Q} is not an observable quantity and not a Lorentz invariant in general relativity, however it is a measure of the total amount of energy converted from neutrinos to e^+e^- pairs at all radii. With this quantity we wish to measure the total amount of local energy deposited via $\nu\bar{\nu} \rightarrow e^+e^-$ and thus available for neutrino-electron scattering or other such energy exchange processes. For this quantity we get

$$\begin{aligned} \dot{Q} &= \int_R^\infty \dot{q} 4\pi r^2 dr \sqrt{1-2Mr} \\ &= 28G_F^2\pi^6\zeta(5)3c^5h^6 \left(k\sqrt{\frac{7}{4}\pi ac} \right)^9 DL_\infty^{9/4} \left((1-2MR)^{3/2}R \right)^{3/2} \\ &\times \int_1^\infty (x-1)^4(x^2+4x+5)y^2dy(1-2MyR)^5 , \end{aligned} \quad (23)$$

where x is defined by Equation (16) and $y \equiv rR$. This becomes

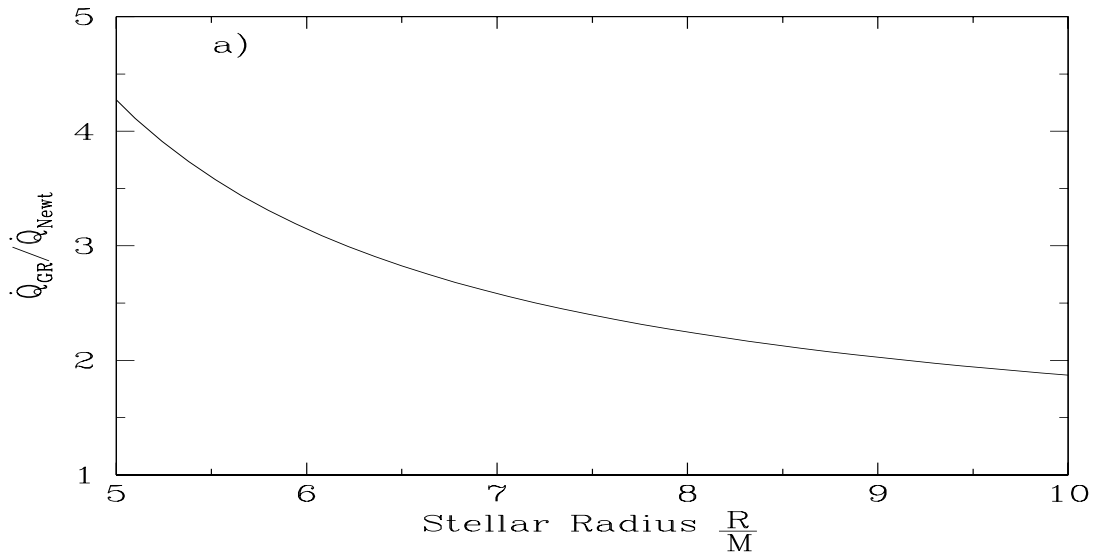
$$\dot{Q}_{51} = 1.09 \times 10^{-5} \mathcal{F}(MR) DL_{51}^{9/4} R_6^{-3/2}, \quad (24)$$

where \dot{Q}_{51} and L_{51} are in units of 10^{51} ergs/sec, R_6 is the radius in units of 10 km, and we have defined

$$\mathcal{F}(MR) \equiv 3(1 - 2MR)^{9/4} \int_1^\infty (x - 1)^4 (x^2 + 4x + 5) y^2 dy (1 - 2MyR)^5. \quad (25)$$

For the Newtonian case, $\mathcal{F}(0) = 1$, and we recover the result found in Cooperstein, van den Horn & Baron (1986). Note that Equation (24) is for only a single neutrino flavor. Hence, Equation (3) must be evaluated and L_{51} must be summed over each neutrino flavor in order to get the total energy deposition due to annihilation of all neutrino flavors.

A key purpose of this paper is to quantify the general relativistic augmentation of local e^+e^- pair energy deposition compared to the Newtonian calculations. In Figure (1) the ratio $\dot{Q}_{GR}/\dot{Q}_{Newt} = \mathcal{F}(MR)$ is plotted over a range of stellar radii R/M . It is somewhat surprising to find that the $\nu\bar{\nu}$ annihilation is enhanced by almost a factor of 2 at the rather large radius $R = 10M$, increasing to a factor of 4 at $R = 5M$. As will be discussed, this is the relevant range for type II supernova models. In the more extreme relativistic regime, down to $R = 3M$, pertinent to collapsing neutron stars, this enhancement rises to nearly a factor of 30.



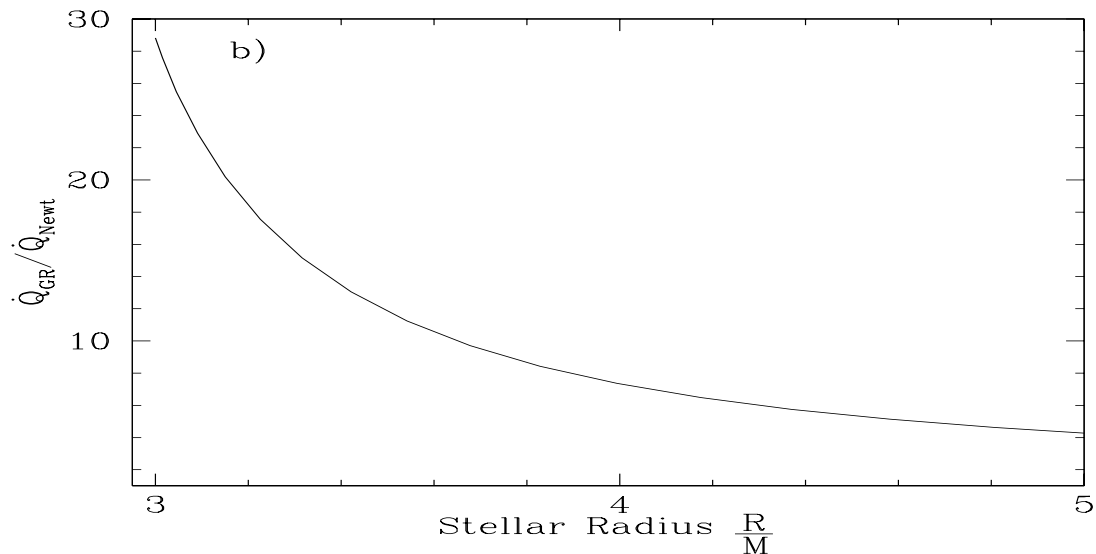


Fig. 1.— Ratio of general relativistic energy deposition \dot{Q}_{GR} to total newtonian energy deposition \dot{Q}_{Newt} around a neutron star as a function of neutron star neutrinosphere radius **a)** in the range relevant to supernovae **b)** and the more extreme relativistic range, down to $R = 3M$, relevant to collapsing neutron stars.

In order to show this enhancement as a function of radius, Figure (2) plots $d\dot{Q}dr$ for several stellar masses MR . As expected, the enhancement is strongest near the surface of the neutron star. Thus the overall efficiency of this process will be dependent upon the conditions near the surface of the neutron star such as scale-height of the baryonic atmosphere. This point will be important in the discussion of supernovae.

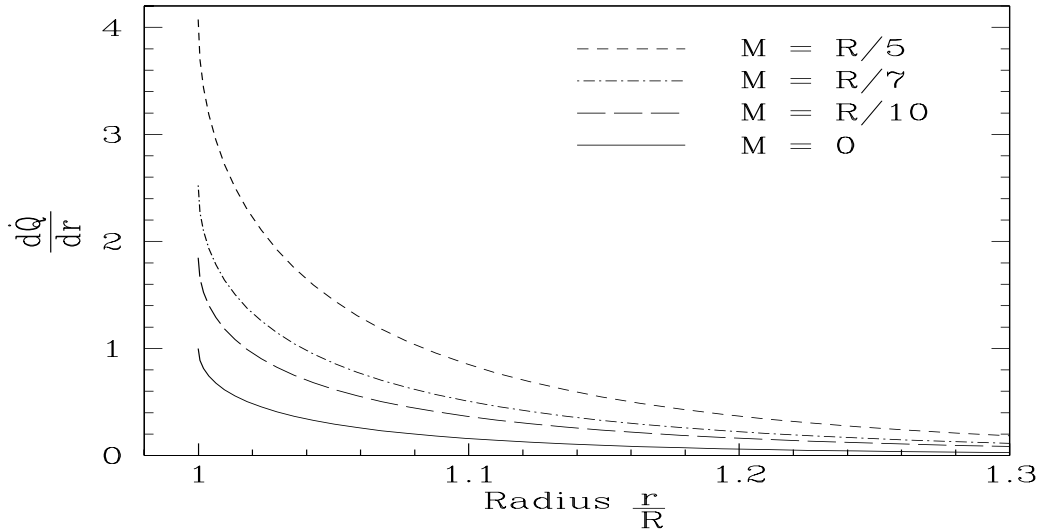


Fig. 2.— $d\dot{Q}/dr$ for various stellar masses MR . Neutrino pair annihilation efficiency drops off rapidly with radius. Curves are normalized such that the Newtonian case $M = 0$ is 1 at $r = R$.

The enhancements discussed here are the result of two different relativistic effects. The first is path bending of neutrinos emanating from the neutron star neutrosphere. The $\nu\bar{\nu}$ annihilation cross-section varies like the square of the center-of-mass energy and thus favors head-on $\nu\bar{\nu}$ collisions. A simple interpretation of the effect of path bending from Equation (14) is that it increases the apparent angular size of the star as seen by a neutrino at radius r . This increases the number of near-horizontal neutrinos and thus the probability of head-on collisions.

The second effect is that of gravitational redshift. As the neutrinos rise above the surface of the neutron star, they cool. Since $\nu\bar{\nu}$ annihilation depends strongly on energy; $\dot{q} \propto T^9$ as in Equation (8), the annihilation efficiency is strongly reduced by nine powers of redshift. However, the energy of neutrinos at the neutrosphere of the star is not directly observable. Only the neutrinos at infinity are measured. Thus \dot{q} is put in terms of an observed luminosity L_∞ in Equation (22). The gravitational field, then, requires a greater photosphere luminosity $L(R)$ for a given observed luminosity L_∞ . For an observed L_∞ there is a net gain in \dot{q} at the neutrosphere relative to a Newtonian calculation. It is worthwhile to note that this effect is important to all luminosity dependant processes near a neutron star, not just $\nu\bar{\nu}$ annihilation.

5. Discussion

The simple analytical arguments presented here are meant to illustrate and quantify the importance of general relativity in the physics of emission from compact, massive objects. The physics near the surface of a hot ($T \sim \text{MeV}$) neutron star is extremely complex, with all possible interactions between baryons, leptons, photons and neutrinos playing important roles in energy conversion and transport. Here we have considered only one process: $\nu + \bar{\nu} \rightarrow e^+ + e^-$. This is clearly only a small component of a complete model of the many processes involved.

However, the reaction considered here is of particular importance in tapping the tremendous neutrino flux emanating from a hot neutron star. Quantifying the dependance of this reaction on gravity is crucial to understanding the ultimate energy transport from a radiating neutron star.

The present paper considers two problems in astrophysics for which the efficiency of the reaction $\nu + \bar{\nu} \rightarrow e^+ + e^-$ near the surface of a hot neutron star is important: supernovae and close neutron star binaries. A discussion of each in turn follows.

5.1. Supernovae

Figure (3) shows the evolution of the protoneutron star radius during a Type II supernova, starting from initial collapse, as calculated by the Wilson-Mayle supernova code (Wilson & Mayle 1988, Mayle & Wilson 1989). It is evident that the protoneutron star shrinks rapidly for a couple of seconds. This contraction finally halts at a radius of about 10 km. The density scale-height at the surface of the protoneutron star neutrinosphere is indicated in figure (3) by $|d \log \rho d \log r|$. As the star contracts and gravity becomes stronger, the photosphere becomes more sharply defined. Thus we expect the protoneutron star surface to converge to the idealized neutrinosphere model considered here.

In order to explore this idea we define an angular cutoff factor as in Cooperstein, van den Horn & Baron (1987):

$$\chi_{Newt}(r) = 18(x - 1)^2(x^2 + 4x + 5) , \quad (26)$$

where x is defined by Equation (16) with $M = 0$. $\chi_{Newt}(r)$ is related to $\Theta(r)$ of Equation (17), but only contains relative neutrino direction information $\sim (1 - \mathbf{\Omega}_\nu \cdot \mathbf{\Omega}_{\bar{\nu}})^2$ and is normalized such that $\chi = 1$ for an isotropic neutrino distribution. Wilson and Mayle have evaluated the cutoff factor, χ_{W-M} , in their supernova code by solving the Boltzmann equation at various times assuming density, temperature and electron fraction are fixed

functions of radius. Figure (4) shows a comparison between the neutrino beaming from an idealized Newtonian photosphere and that calculated by the Wilson-Mayle supernova code. At early times, 0.2 seconds after the bounce, the baryon extended atmosphere scatters the neutrinos above the photosphere, thus rendering the neutrino angular distribution more isotropic than is the case for an idealized sharp neutrinosphere. At early times, $t < 0.5$ seconds, this effect of scattering overshadows any effect due to bending and thus simple neutrino bending is not a valid model for these times.

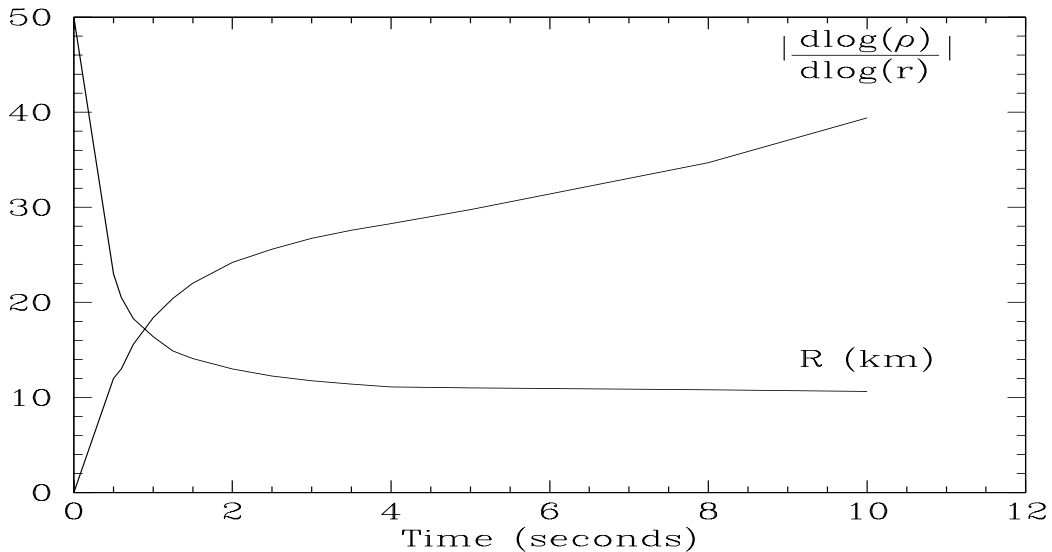


Fig. 3.— The evolution of a $1.41M_{\odot}$ ($= 2.1$ km) protoneutron star as calculated by the the Wilson-Mayle supernova code is characterized by rapid shrinkage to a radius $R \approx 10$ km and a strong steepening of density profile at the photosphere as indicated by $|d \log \rho d \log r|$.

After about one second the protoneutron star radius has contracted to less than 20 km and its surface has become much more sharply defined, with a baryon atmosphere scale-height ~ 100 meters. Thus the calculations exhibited here are valid for $R \lesssim 20$ km when the star surface has converged sufficiently toward a sharp boundary and neutrino-baryon scattering is minimized. We conclude that after about one second general relativistic effects are important to the dynamics of a supernova. In particular, at late times, ~ 10 seconds after the bounce, the matter that will ultimately be involved in the r-process is being ejected from the protoneutron star. The heating of the ablated matter in relativistic wind calculations (Cardall & Fuller 1997) will be greatly enhanced over newtonian wind calculations (Woosley et al. 1994).

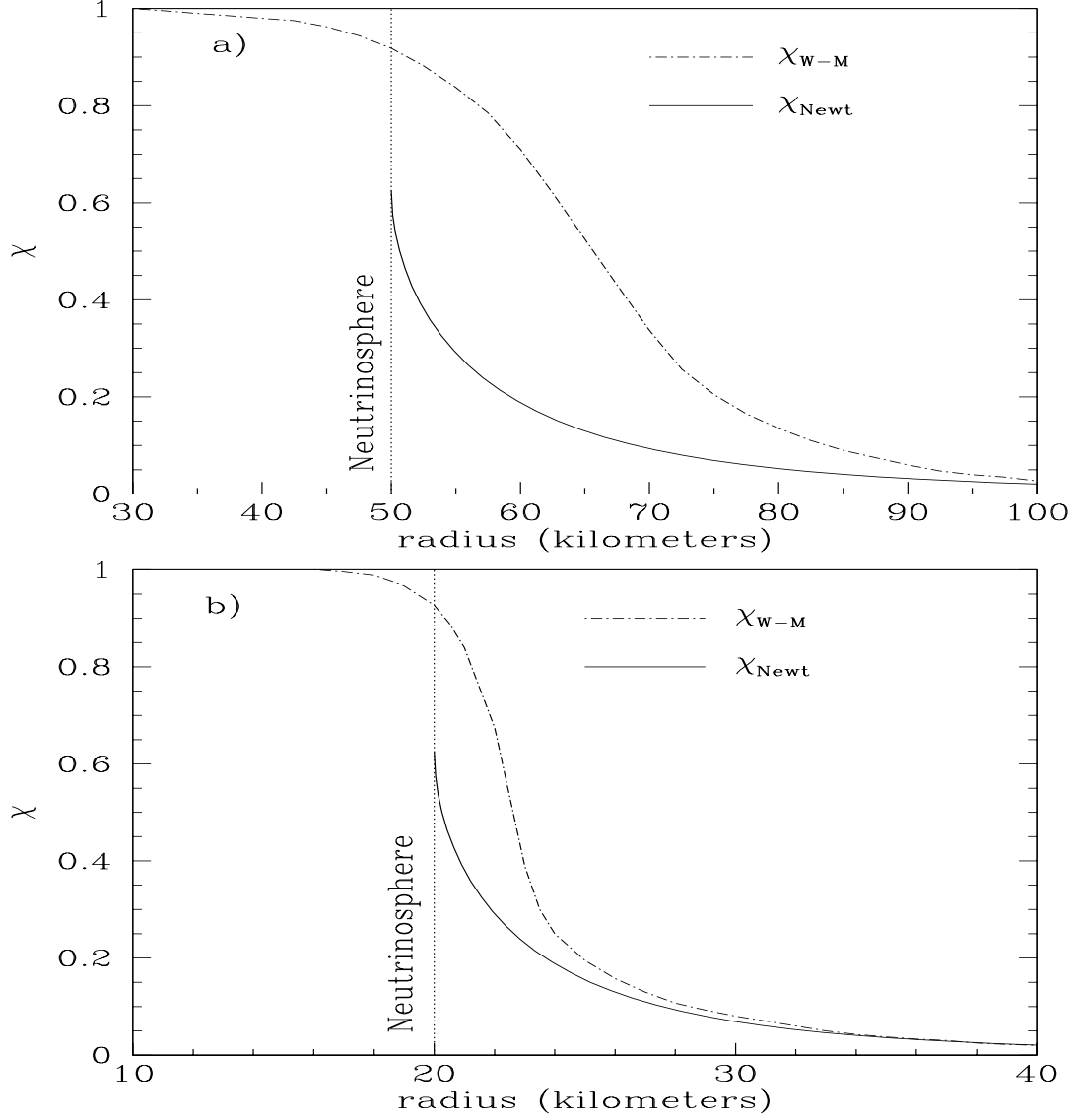


Fig. 4.— Comparison of angular cutoff factor χ_{W-M} obtained from the Wilson-Mayle supernova code with that of the Newtonian calculation χ_{Newt} from Equation (26). As the star shrinks through **a)** radius $R = 50$ km at time $t = 0.2$ seconds after collapse and **b)** $R = 20$ km at $t = 0.5$ seconds, the surface becomes more sharply defined and better approximated as a smooth neutrinosphere.

5.2. Close Neutron Star Binaries

Recent numerical calculations of neutron stars in close binary systems near their last stable orbit have indicated that the stars may experience a relativistic compressive force and subsequent heating (Wilson et al. 1996, Mathews & Wilson 1997, Mathews, Marronetti & Wilson 1998). It is argued that 0.5×10^{53} ergs per star of thermal neutrinos might be released within a few seconds. This may be a viable engine for gamma-ray bursts (Wilson, Salmonson, & Mathews 1997; 1998). Accurately understanding the efficiency of conversion from neutrinos to other forms of matter (i.e. e^+e^- pairs) is crucial to predicting the possible gamma-ray burst characteristics. As shown in Figure (1), the relativistic enhancements of the reaction $\nu\bar{\nu} \rightarrow e^+e^-$ for a compact neutron star in a binary can be large; up to a factor of 30 for $R = 3M$. The calculations of Wilson et al. 1996 indicate that $R \approx 3M$ is the radius at which the neutrons stars collapse to black holes. Such large enhancements of this reaction rate must be taken into account when modeling the emission from a hot, compressed neutron star. Since at late time the neutrino luminosity rises to $\sim 10^{53}$ ergs/second, we estimate that such enhancements will allow more than 10% of the energy emitted in neutrinos to be converted to e^+e^- pairs. This estimate includes electron scattering of the neutrinos by the annihilation-produced pairs, which will more than double the energy deposition rate. This energy in e^+e^- pairs can then go on to generate a gamma-ray burst.

6. Conclusions

We have shown that the strong gravity near the surface of a neutron star requires a relativistic treatment when modeling stellar emission. In particular, when considering the reaction $\nu\bar{\nu} \rightarrow e^+e^-$ the effects of path bending and redshift can enhance the efficiency by up to a factor of 4 for $R = 5M$ relevant for the proto-neutron star at late-times in a type II supernovae. A factor of 30 is possible for $R = 3M$ relevant to collapsing neutron stars. These calculations on their own are incomplete when considering the total emission from a neutron star; one must perform computations including all relevant processes. However, these calculations indicate that relativistic effects will enhance the e^+e^- pair energy from the neutrino luminosity emanating from the neutron star. This added e^+e^- pair energy is important for modeling late-time supernovae and for gamma-ray bursts from collapsing neutron stars. Thus general relativistic computations are necessary for the accurate modeling of neutrino winds from neutron stars.

Work performed under the auspices of the U.S. Department of Energy by the Lawrence Livermore National Laboratory under contract W-7405-ENG-48.

REFERENCES

- Bhattacharya, D. & van den Heuvel, E. P. J. 1991, *Phys. Rep.*, 203, 1
- Bethe, H. A. 1990, *Rev. Mod. Phys.*, 62, (4), 801
- Bethe, H. A. & Wilson, J. R. 1985, *ApJ*, 295, 14
- Cardall, C. Y., Fuller, G. M. 1997, *ApJ*, 486, L111
- Cooperstein, J., van den Horn, L. J., and Baron, E. 1986, *ApJ*, 309, 653
- Cooperstein, J., van den Horn, L. J., and Baron, E. 1987, *ApJ*, 321, L129
- Fryer, Benz, & Herant 1996, *ApJ*, 460, 801
- Goodman, J., Dar, A., and Nussinov, S. 1987 *ApJ*, 314, L7
- Mathews, G. J., Marronetti, P., Wilson, J. R. 1998, *Phys. Rev. D*, 58, 043003
- Mathews, G. J., Wilson, J. R. 1997, *ApJ*, 482, 929
- Mayle, R. & Wilson, J. R. 1989, *ApJ*, 334, 909
- Misner, C. W., Thorne, K. S., Wheeler, J. A. 1975 *Gravitation* (New York:Freeman), 673
- Wilson, J. R., Mathews, G. J. & Marronetti, P. 1996, *Phys. Rev. D*, 54, 1317
- Wilson, J. R. & Mayle R. 1988, in *Proceedings of the Fifth Marcel Grossmann Meeting on General Relativity*, ed. D. G. Blair & M. J. Buckingham (Singapore:World Scientific), 217
- Wilson, J. R., Salmonson, J. D., Mathews, G. J. 1997, in *AIP Conf. Proc. 428 Gamma-Ray Bursts: 4th Huntsville Symposium*, ed. C. A. Meegan *et al.* (New York:AIP), 788
- Wilson, J. R., Salmonson, J. D., Mathews, G. J. 1998, in *2nd Oak Ridge Symposium on Atomic and Nuclear Astrophysics* ed. A. Mezzacappa (Philadelphia:IOP), 705
- Woosley, S. E., Wilson, J. R., Mathews, G. E., Hoffman, R. D., Meyer, B. S. 1994, *ApJ*, 433, 229